

Modeling and effect of the anomaly of a ball rolling on the stability of the induction machine operating

Néjib Khalfaoui ¹, Salhi Mohamed Salah ², Hamid Amiri ³

¹(LR SITI, ENIT/ ISET Of JENDOUBA, Tunisia)

²(LR SITI, ENIT / SAAT MATEUR, Tunisia)

³(Director LR SITI Lab, ENIT /ENIT, Tunisia)

Abstract: *This paper deals with statistics related to the distribution of causes of anomalies affecting the induction machines and in particular ball rolling, besides presenting the kinematic anomalies characteristic frequencies of the rolling elements. It also presents a mathematical modeling of the anomaly (indentation) on the outer ring and inner ring of the ball rolling. In this paper, we do not only do a spectral analysis of the transmitted signal, but also we study the effects of the anomaly on the electrical quantities (stator currents) and mechanical quantities (load torque) as well as its spread between the elements of the machine and the structure of the resonance phenomenon that appears around specific frequencies, particularly the effect of the anomaly on the stability of the operating of the machine. Also a simulation performed by matlab with spectral analysis and an experimental monitoring by vibration analysis in the laboratory of NDC (Non Destructive Control) will be the object of a more synthetic analysis.*

Keywords: *Anomaly modeling, Induction machine, Rolling anomaly, Spectral analysis, Stability of operating.*

I. Introduction

In many industrial areas, the monitoring and the diagnosis of the systems play an important role and allow to know the types of the origins of defects that can affect the systems. Indeed, the electrical drive systems based on induction machine are widely used in industrial applications thanks to their low cost, their performance and robustness. In fact, this induction machine is omnipresent in many applications, particularly in high-tech sectors such as aerospace, nuclear, chemical industries, in transport (metro, trains, propulsion of vehicles and ships, elevators), in industry (machine tools, winches), in appliances. It was originally used only in motor but, again thanks to the development of power electronics, it is increasingly often used as a generator, in the case of wind turbines for example. Operating costs, mainly related to maintenance, have been increasing [1]. However, degraded operating modes can occur during the life of the machine. One of the main reasons for these failures remains ball rolling anomalies. To improve the operating safety of machines, monitoring systems can be implemented in order to ensure a preventive and systematic maintenance [2] [3]. In this regard, several studies have been conducted on the reliability of electrical machines made by different industry groups. The main study, conducted by the company "General Electric", was published in EPRI (Electric Power Research Institute) in 1982; It covers about 5000 engines, of which approximately 97% were induction machines. This study shows that the ball rolling anomalies account for about 50% of breakdowns of the induction machine (Fig.1).

Many published researches [2], [3], [4], [5], [6], [7], [8], [9], [10], [11], [12], [13], deal with mechanical anomalies of electrical drive systems based on induction machine, mainly ball rolling defects, but do not have their mathematical modeling either on the outer or inner ring to subsequently analyze their effects on electrical and mechanical quantities of the machine and this is where the very objective of this paper which aims at developing the efficiency of this modeling and the effects of anomalies on the machine. Thus, the creation of vibration measurements to detect mechanical anomalies rolling type requires the use of vibration sensors often piezoelectric type conditioners and data acquisition channels. In addition, the spatial positioning of the sensors must be studied according to the mechanical member to be monitored. As part of the electrical workouts based induction machine, many researches have been conducted to replace the detection of mechanical anomalies based on the measurement of vibration magnitudes, by detection based on the measurement of electrical quantities, such as stator currents of the machine [4]. Furthermore, the stator currents of the induction machine are often already measured for the control and protection devices.

II. Heading s Statistical study of the induction machine anomalies

Anomalies can be of various origins: electrical, mechanical, thermal, environmental or even magnetic. Their causes are multiple and can be classified into three groups [3] [4]:

- 1) Failure generators or anomaly initiators: engine overheating, electrical fault (short circuit), power boost, electrical insulation problem, wear of mechanical parts (ball rolling), fixations breaking, etc.

- 2) Faults amplifiers: frequent overloading, mechanical vibrations, wet environment, continuous heating, poor lubrication, aging, etc.
- 3) Manufacturing defects and human errors: manufacturing defects, defective parts, inadequate protections, bad sizing of the machine, etc [1].

The distribution of defects in the different parts of the engine is shown in Fig.1:

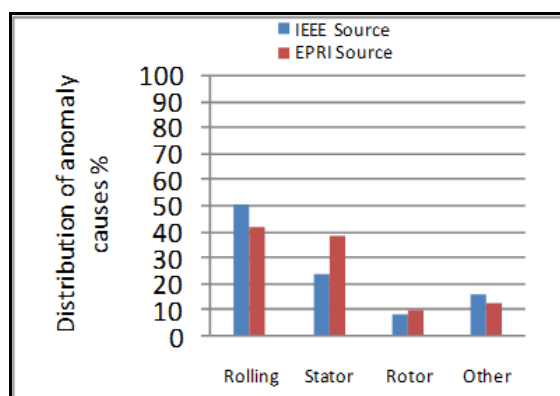


Fig.1: Distribution of anomaly causes in induction machines

The mechanical constraints are high, which explains the high rate of failure entailed by rolling [2]. These require an increased mechanical maintenance.

III. Mechanical Defects

1. Rolling anomalies

The ball rolling act as an electromechanical interface between the stator and the rotor. In addition, they represent the holding element of the machine axis, allowing to ensure a proper rotation of the rotor. Most faults occur in rolling of induction motors as well as the reasons of their aging. This kind of fault is most common in medium and high power machines. It is usually related to rolling wear and specifically beads degradation, or tread. Their possible causes are [1][5][6]:

- Wear due to aging,
- High operating temperature,
- Loss of lubrication,
- Contaminated oil
- Mounting defaults
- Tree currents (Shaft Current)

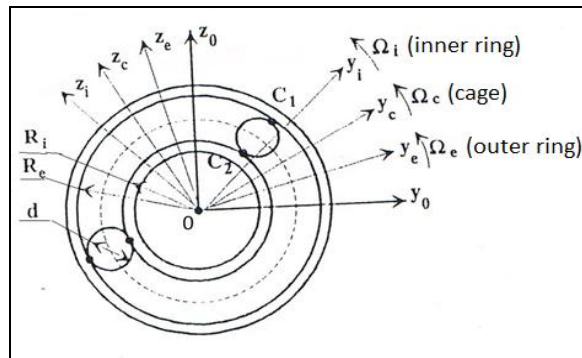
The direct consequences of this failure on the rolling are:

- Holes in the inner and outer raceway grooves.
- The ripple of their tread.
- Corrosion due to water.
- Lubrication fault problem due to the temperature.
- Separation, surface erosion caused by overload.

For the system, this type of defect results in oscillations of the load torque, additional losses and a clearance between the inner ring and the outer ring of the rolling causing vibrations coming from displacements of the rotor around the longitudinal machine axis. In the worst case, the presence of a defective rolling can lead to engine lock

2. Modeling of rolling anomalies

Consider a rolling in a fixed reference (Oy₀z₀) [1] [6] [7].



d: ball diameter; Ω: angular velocity
 Re: outer radius; Ri: inner radius

Fig.2: Repositories related to a rolling element

2.1. kinematic frequencies:

Defects, cracks, flaking etc..... may exist on the inner rings, outer, on the balls; they generate shock, so the periodic vibrations when the rotational speeds are constant.

The fundamental frequencies of these vibrations are related to the so-called basic kinematic frequencies:

f_c: the cage rotation frequency compared to a fixed reference.

$$f_c = \frac{\Omega_c}{2\pi} \tag{1}$$

f_b: rotational frequency of an element with respect to an axis passing through its center:

$$f_b = \frac{\Omega_b}{2\pi} \tag{2}$$

The speeds of relative displacements null at C1 and C2 contact points. Using the frequencies f_i of rotation of the inner ring, f_e of the outer ring and the contact angle α, the cage frequency f_c expressed as:

$$f_c = \frac{1}{2} \left(1 - \frac{d \cos \alpha}{Dm} \right) f_i + \frac{1}{2} \left(1 + \frac{d \cos \alpha}{Dm} \right) f_e \tag{3}$$

By introducing the frequency and angle α contact, the ball frequency f_b is expressed as :

$$f_b = \frac{1}{2} \frac{Dm}{d} |f_e - f_i| \left(1 - \frac{d \cos \alpha}{Dm} \right) \left(1 + \frac{d \cos \alpha}{Dm} \right) \tag{4}$$

Forms 3 and 4 define the basic kinematic frequencies (cage and ball) from the rotation frequencies of the f_i inner and f_e outer rings.

At frequencies f_c and f_b base associated defects:

-Frequency of rotation of the cage, cage defects:

$$f_{cagedefects} = f_c = \frac{1}{2} \left(1 - \frac{d \cos \alpha}{Dm} \right) f_i + \frac{1}{2} \left(1 + \frac{d \cos \alpha}{Dm} \right) f_e \tag{5}$$

- Rotation frequency of a rolling element; Z number of rolling elements:

$$f_{element} = f_b = \frac{1}{2} \frac{Dm}{d} |f_e - f_i| \left(1 - \left(\frac{d}{Dm} \right)^2 \cos^2 \alpha \right) \tag{6}$$

-Frequency due to a defect on the inner ring:

$$f_{inner\ ring} = f_{b,int} = \frac{Z}{2} |f_i - f_e| \left(1 + \frac{d}{Dm} \cos \alpha \right) \tag{7}$$

-Frequency due to a defect on the outer ring:

$$f_{outer\ ring} = f_{b,ext} = \frac{Z}{2} |f_e - f_i| \left(1 - \frac{d}{D_m} \cos \alpha \right) \quad (8)$$

In keeping with calculating arrangements, research works and industrial experts have the following expressions

$$f_b = \frac{f_r D_m}{2 d} \left[1 - \left(\frac{d \cos \alpha}{D_m} \right)^2 \right] \quad (9)$$

$$f_c = \frac{f_r}{2} \left(1 - \frac{d \cos \alpha}{D_m} \right) \quad (10)$$

$$f_{b\ int} = \frac{f_r}{2} Z \left(1 + \frac{d \cos \alpha}{D_m} \right) \quad (11)$$

$$f_{b\ ext} = \frac{f_r}{2} Z \left(1 - \frac{d \cos \alpha}{D_m} \right) \quad (12)$$

With:

- f_r is the rotor rotation frequency
- f_b is the rotational frequency of the ball
- f_c is the cage rotation frequency
- $f_{b\ int}$ the rotational frequency of the inner ring
- $f_{b\ ext}$ the rotational frequency of the outer ring
- Z is the number of balls
- d is the ball diameter
- D_m is the average diameter of the rolling
- α is the contact angle.

2.2. Modeling anomaly on the outer ring:

Suppose chipping (indentation) of small size; the passage of a ball on this peeling causes a force in a radial plane perpendicular to the rotation line with a contact angle α Fig.3 [1][7][12]:

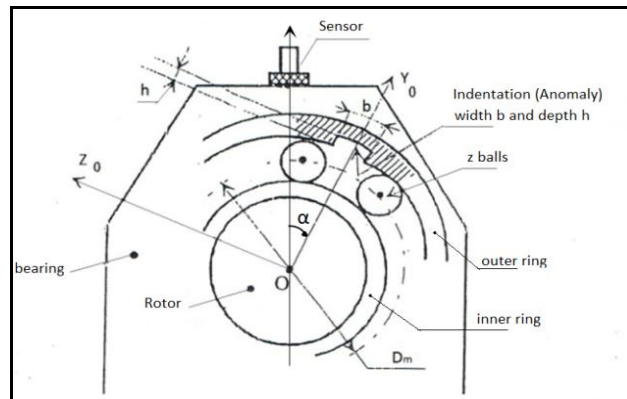


Fig.3: Anomaly on the fixed outer ring

The set of rolling elements causes a series of pulses described in a fixed reference frame (Ox_0y_0) by a line series; the pulse frequency is equal to f_{bext} :

$$SHA_{1/f_{bext}} = \sum_{k=-\infty}^{\infty} \delta \left(1 - \frac{k}{f_{bext}} \right) \quad (13)$$

With SHA : Dirac distribution

These assumptions allow relatively simple mathematical developments to.

A rotating force to the speed ($2\pi f_r$) of the rotor due to an imbalance, an arrow, to a defect of coaxiality. The turning force causes a variation in the force between the rolling element and the fault, this force models pulse amplitude of the series.

The radial force, applied in the stead of the anomaly, is written:

$$f(t) = A(1 + \gamma \cos 2\pi f_r t) \cdot SHA_{1/f_{bext}}(t) \quad (14)$$

with γ is the rate modulation.

The signal $h(t)$ output from the sensor disposed on the structure of Fig.3 in a radially pulse applied to the right defect the pulse comb signal is:

$$S(t) = h(t) * f(t) \Leftrightarrow S(v) = H(v).F(v) \tag{15}$$

v frequency : $-\infty < v < \infty$
 $H(v)$: transfer function of sensor structure

$$F(v) = A \left(\delta(v) + \frac{\gamma}{2} [\delta(v - f_r) + \delta(v + f_r)] \right) * (f_{bext} \cdot SHA_{fbext}(v)) \tag{16}$$

$$SHA_{fbext}(v) = \sum_{m=-\infty}^{\infty} \delta(v - mf_{bext}) \tag{17}$$

With δ : Dirac distribution

$$S(v) = A \cdot f_{bext} \cdot H(v) \cdot \left[\begin{array}{l} SHA_{fbext}(v) + \frac{\gamma}{2} SHA_{fbext}[v - (kf_{bext} - f_r)] \\ + \frac{\gamma}{2} SHA_{fbext}[v - (mf_{bext} + f_r)] \end{array} \right] \tag{18}$$

The $SHA_{fbext}(v)$ comb repeats the frequency f_{bext} the Dirac distribution $\delta(v)$ for $v = 0$ (convolution). The comb $SHA_{fbext}[v - (kf_{bext} - f_r)]$ result of the convolution by $\delta(v + f_r)$ by $SHA_{fbext}(v)$, and for $SHA_{fbext}[v - (mf_{bext} + f_r)]$.

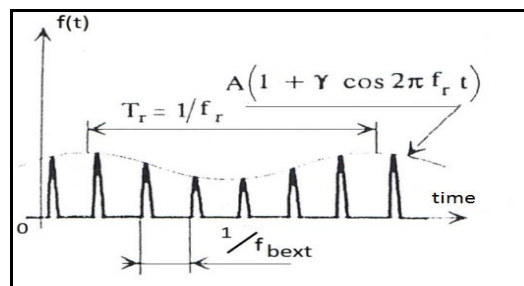


Fig.4: Radial force applied to the right defect.

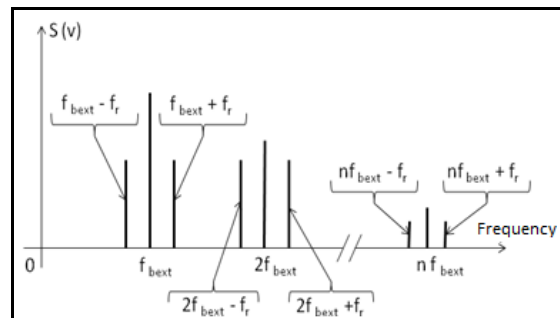


Fig.5: Spectrum S(v)

In fact, the spectrum $S(v)$ contains components whose frequencies are defined by fig.5. We note that the impulsiveness of excitation introduced nf_{bext} components to higher frequencies ; nf_{bext} ; $nf_{bext} \pm f_r$, when the pulses are not Dirac distributed pulses, the components of the pulses become negligible as n increases. $nf_{bext} \pm f_r$; in deed, the faults are represented by periodic pulses of finite length, which does not substantially alter the components $nf_{bext} \pm f_r$.

2.3. Modeling anomaly on the rotating inner ring .

If we consider the indentation to small size, the passage of a rolling element on this indentation causes a force in a radial plan perpendicular to the rotation line [1] [3] [7]. This force is in a repository ($ox_i z_i$) in rotation speed Ω ; its frequency is equal to f_{bint} (Fig. 6).

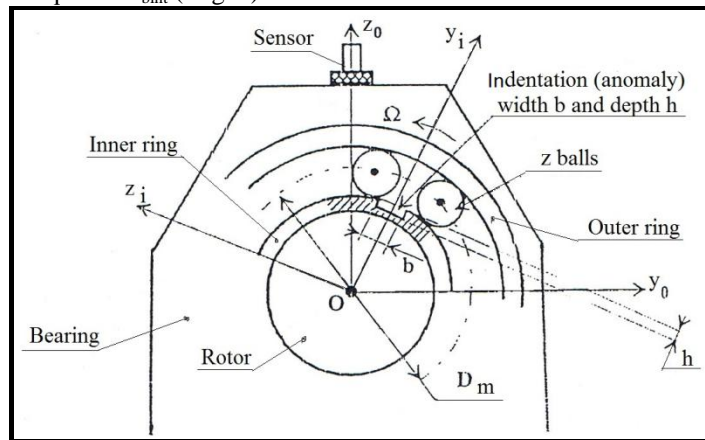


Fig.6 : Anomaly on the inner ring

The anomaly in rotation speed $\Omega = 2\pi f_r$ rotor encounters a zone between ϑ_1 and ϑ_2 in which the radial load is not zero (Fig.7).

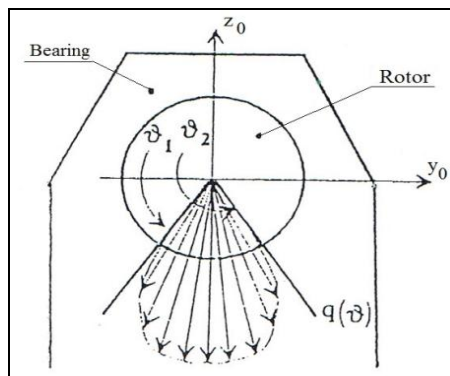


Fig.7 : Radial load between ϑ_1 and ϑ_2

The anomaly due to the indentation in the rotating reference imposes a radial force $f(t)$ represented by a series of pulses (Fig.8), the ratio τ_d/T_d is independent of Ω . This force meets the radial load $q(t)$ defined in Fig. 9.

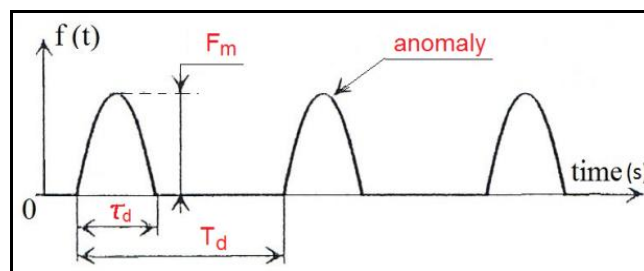


Fig.8 : Form of the radial force

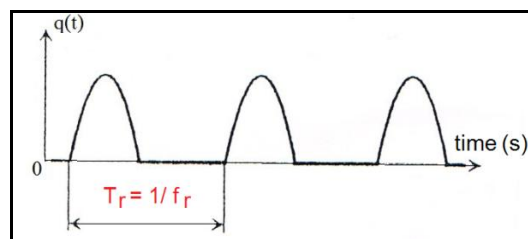


Fig.9 : Form of the radial load

In the fixed reference (ox_0z_0) the radial force $f_{radiale}(t)$ is defined by the following expression:

$$f_{Radiale}(t) = q(t) \cdot \text{SHA}_{f_{b\text{int}}}^{\pm}(t) * \text{SHA}_{f_r}^{\pm}(t) \tag{19}$$

With SHA : Dirac distribution

The application management point of the radial force on the fixed structure varies over time in the speed $\Omega = 2\pi fr$ This can result in a transfer function whose input varies with the speed of rotation and thus modulates average transfer function associated to an impulse response $h_o(t)$.

$$h(t) = h_o(t) [1 + \gamma_1 \cos 2\pi f_r t] \tag{20}$$

The sensor output signal may be written:

$$S(v) = h(v) * f_{Radiale}(v) \iff S(v) = H(v) \cdot F_{Radiale}(v) \tag{21}$$

With:

$$H(v) = H_0(v) * \left\{ \delta(v) + \frac{\delta_1}{2} [\delta(v - f_r) + \delta(v + f_r)] \right\} \tag{22}$$

And

$$F_{Radiale}(v) = [f_{b\text{int}} \cdot Q(v) * \text{SHA}_{f_{b\text{int}}}(v)] \cdot [f_r \cdot \text{SHA}_{f_r}(v)] \tag{23}$$

Then :

$$S(v) = \left[H_0(v) * \left\{ \delta(v) + \frac{\delta_1}{2} [\delta(v - f_r) + \delta(v + f_r)] \right\} \right] \cdot [f_r \cdot f_{b\text{int}} \cdot Q(v) \cdot \text{SHA}_{f_r}(v) * \text{SHA}_{f_{b\text{int}}}(v)] \tag{24}$$

-The First term in equation:

$$H_0(v) * \left\{ \delta(v) + \frac{\delta_1}{2} [\delta(v - f_r) + \delta(v + f_r)] \right\} = H_0(0) + \frac{\delta_1}{2} [H_0(f_r) + H_0(-f_r)] \tag{25}$$

This term is independent of the frequency; within the meaning of frequencies it does not alter the spectrum ($kf_{b\text{int}} \pm qf_r$) resulting from the second factor . To avoid overlapping, it is necessary that the spectral width of $Q(v)$ is lower to $f_{b\text{int}}$.

- The second term of the equation :

- the term $Q(v) \cdot \text{SHA}_{f_r}(v)$ defines a discretization frequency f_r of the Fourier Transform of the radial load $q(t)$.
- the term $[Q(v) \cdot \text{SHA}_{f_r}(v)] * \text{SHA}_{f_{b\text{int}}}(v)$ defines a periodization at frequency $f_{b\text{int}}$ from a $Q(v)$. $\text{SHA}_{f_r}(v)$ discrete (figure5);This spectrum contains components at frequencies: $kf_{b\text{int}} \pm qf_r$: $k, q = 1, 2, 3, \dots$

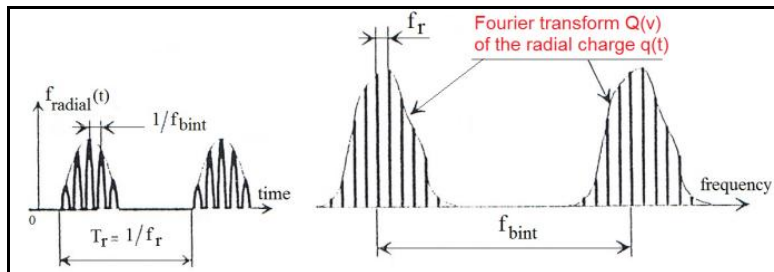


Fig.10 : Spectrum components of the anomaly

IV. Effect of anomaly " indentation " of the inner ring on size electrical and mechanical .

Anomaly rolling the induction machine causes failures depending on how the torque is exerted mechanical load , it can be destructive to the mechanical parts[6], [8], [11], . Poor working conditions can lead to faulty mechanical loads causing :

- Torque jerk ,
- On the couples ,

- A mechanical balance load and torque oscillations ,
- Unbalance phenomena
- Misalignment of rotating shafts

These failures can be classified into two main families :

- the first failure of family succession creating a mechanical eccentricity.
- the second concerns the load torque becomes disrupted.

That during this anomaly will be transferred to the rotor current via the gap permeance and the mechanical position of the rotor , on the other hand the rotor flux will transmit this discrepancy to the stator current .

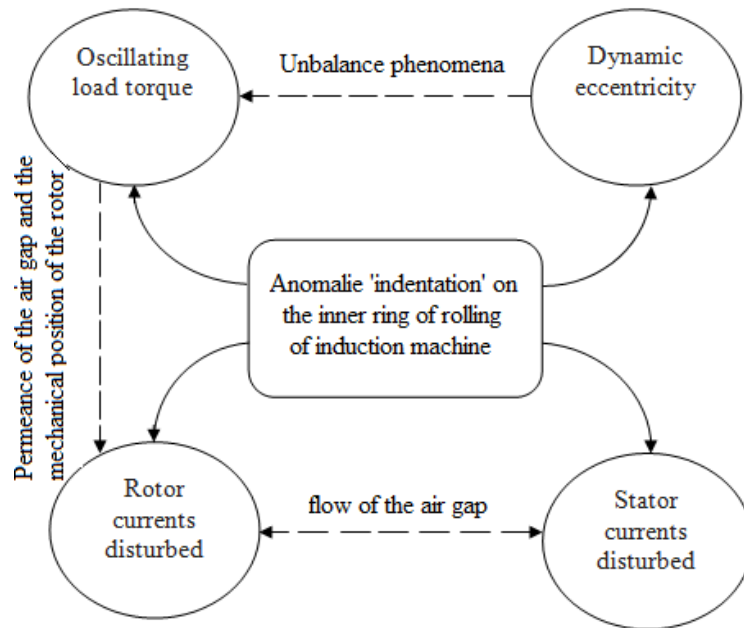


Fig.11: Transfer of anomaly in electrical and mechanical quantities

V. Effects of anomaly “indentation” in the inner ring on the load torque

During the running rotation having an anomaly indentation on the inner ring , there are shocks causing vibrations but also the torque jolts that are repeated periodically in time by inducing oscillations of load torque (Fig. 6) which are measured by a torque meter[4]. Fig. 7 shows a reduced frequency range of the load torque spectrum comparing the harmonic content for a healthy machine and a machine with a rolling with localized anomaly on the inner ring[13], [18]. The rotation speed is nominal, is close to 25Hz .

The expression of the load torque (26) may be represented by a DC component C_0 amplitude equal to the electromagnetic torque C_{em} of the machine and by a series of n harmonic C_n amplitude and pulsation ω_n for anomaly rolling [8] [11] [19].

$$C_{charges}(t) = C_0 + \sum_n C_n \cos(\omega_n t) \quad (26)$$

The load torque is also expressed in the frequency domain by the following expression :

$$TF[C_{charges}(t)] = C_0 \delta(t) + \frac{C_n}{2} [\delta(f - f_n) + \delta(f + f_n)] \quad (27)$$

With: $f_n = f_{osc}$ frequency of oscillation

In this approach, the viscous friction bearings will be neglected, only the inertia of the rotor being considered . The difference between the electromagnetic torque and the load torque is applied to the inertial mechanical system that constitutes the rotor of the machine. Thus, the equation of the mechanical model of the machine is given by the following expression:

$$\Omega(t) = \frac{1}{J_r} \int_t [C_{em}(\tau) - C_{charge}(\tau)] d\tau \quad (28)$$

With: J_r is the inertia of the rotor
 $\Omega(t)$ angular speed of the rotor

1. Simulation results:

The Fig.12 shows the evolution of load torque versus time and the spectral representation is given in Fig.13, in the presence of an anomaly on the rolling inner ring.

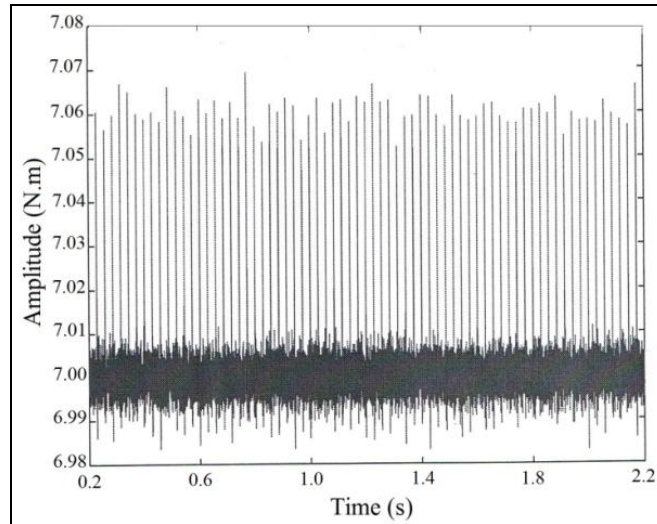


Fig.12: Instant torque of evolution

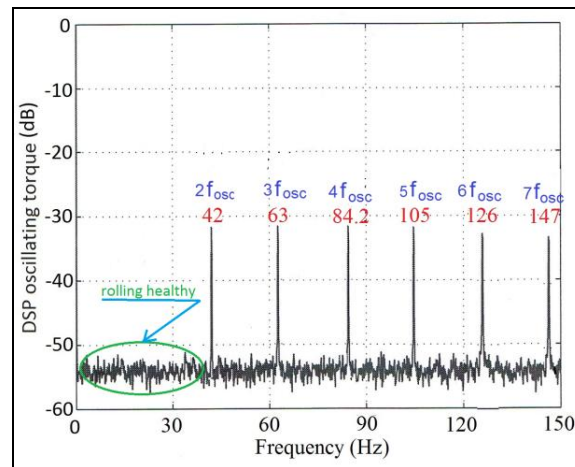


Fig.13 : DSP oscillating torque

1.1. Interpretation:

It may be noted in Figure 13, on the pair of spectra in the presence of an abnormality in the rolling, the occurrence of harmonic lines at frequencies characteristics of anomalies inner ring. However, note that all possible combinations of characteristic frequencies do not exist. Therefore, the spectral content of the load torque on working anomalies can not be predicted completely and theoretically.

VI. Effects of oscillation of the torque on the stator currents

The expression of the angular position (29) of the rotor $\Theta(t)$ of the induction machine also comprises oscillations to the same frequencies f_n .

$$\theta(t) = \theta_0 + \Omega_0 t + \sum_n \frac{c_n}{\omega_n |H(j\omega_n)|} \cos(\omega_n t + \varphi_n) \quad (29)$$

With $H(j\omega_n)$: mechanical transfer function of the machine is assumed to be known

Mechanical position to calculate the magnetomotive force (MMF) rotor which is phase-modulated [3], [12]. Furthermore, the stator MMF is purely sinusoidal. Multiplying these MMF by the airgap permeance considered constant at the angular position and time, leads to the expression of the magnetic field, the integral of this field on the gap surface leads to the magnetic flux and thus the electromotive force (EMF) across one phase temporal tap. Given a linear relationship between the EMF phase current is obtained an expression of the current I_s with the amplitude of the stator current, the amplitude I_r of the rotor current, the fundamental angular frequency ω_s of the stator currents and p the number of pairs of poles of the machine

$$i(t) = I_s \cos(\omega_s t + \phi_s) + I_r \sin[\omega_s t + \sum_n \beta_n \cos(\omega_n t + \phi_n)] \quad (30)$$

With $\beta_n = p \frac{c_n}{\omega_n |H(j\omega_n)|}$

The first term of (30) is related to the contribution of the stator MMF and the second term, phase-modulated, is related to the contribution of MMF rotor. By considering small amplitude phase modulation is obtained a simplified expression of the Fourier transform module (FT) of the current (31) as a function of the frequency f with $f_s = \frac{\omega_s}{2\pi}$ and $f_n = \frac{\omega_n}{2\pi}$.

$$FT\{i(t)\} = (I_s + I_r)\delta(f - f_s) + I_r \sum_n \frac{\beta_n}{2} \delta[f - (f_s \pm f_n)] \quad (31)$$

The appearance of working anomalies can be identified by analyzing the energy variations in frequency components $f_s \pm f_n$ in the current spectrum (fig.20). The β_n parameter is obtained under restrictive conditions as does consider the electromagnetic torque of the constant machine.

VII. Experimental Results

1. Anomaly on the outer ring

The Induction machine on which the experimental tests were carried out presents an anomaly "indentation" of small dimension on the outer ring of the rolling SKF6208 reference.

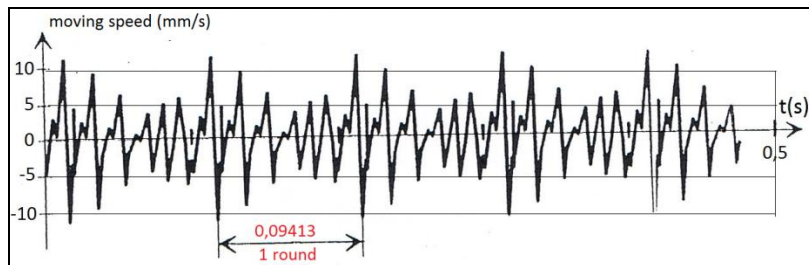


Fig.14: Speed of force movement

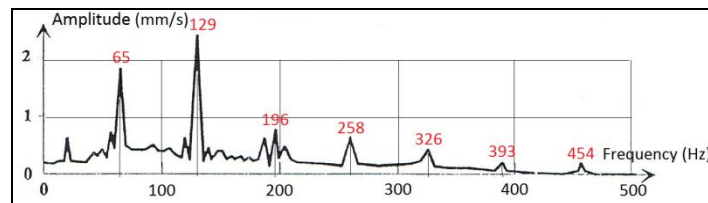


Fig.15: Spectre of vibration amplitude

For simultaneous representation of Fig. 16 spectrum load torque in the case of an anomaly and healthy case showing lines and their frequency characteristics.

The DSP of the torque on the shaft of the machine equipped with a rolling with an anomaly on the outer ring, for a supply frequency $f_s = 50$ Hz machine (rotational frequency of rotor $f_r=25$ Hz). We notice the appearance of harmonics located but focused around a combination of characteristic frequencies. This characteristic of harmonic variations torque amplitudes is due to the anomaly of the rolling.

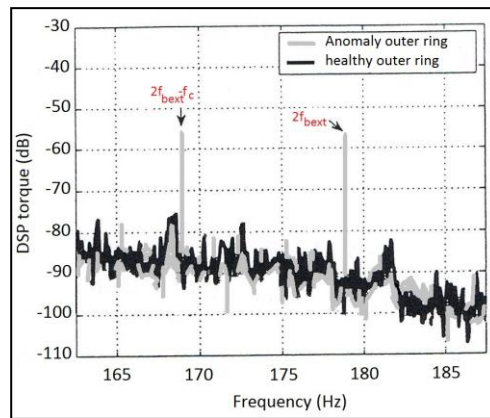


Fig.16: DSP torque for rolling healthy and contaminated

1.2. Interpretation:

The obtained signals given by fig. 14 and 15 show the vibration of a ball rolling, the outer ring is fixed; the rotational speed of the inner ring is equal 630 rev / min

$$f_{bint} = f_r \rightarrow 10,60\text{Hz} \rightarrow 94,13\text{ms} .$$

The spectrum contains lines of: $\approx k \ 65\text{Hz}$; $k = 1, 2, 3, \dots, n$; Theoretical kinematic frequency 65,38Hz differs kinematic measured frequency.

Around the first 3 harmonics, lines at $\pm 8 \text{ Hz}$ are observed. This set of lines expresses a defect on the outer ring and a theoretical frequency of modulation amplitude 65,38Hz.

2. Anomaly on the inner ring

The following results show the vibrations of the ball rolling due to an anomaly ‘‘ indentation’’ on the inner ring of a rotating induction machine speed 1480 rev/ min , the zoom mode around 680.2Hz fig.17, (characterizing the anomaly by the fifth harmonic of the f_{bin} frequency due to an indentation on the inner ring) shows lateral stripes spaced from the rotational frequency (25 Hz) that reflect an amplitude modulation.

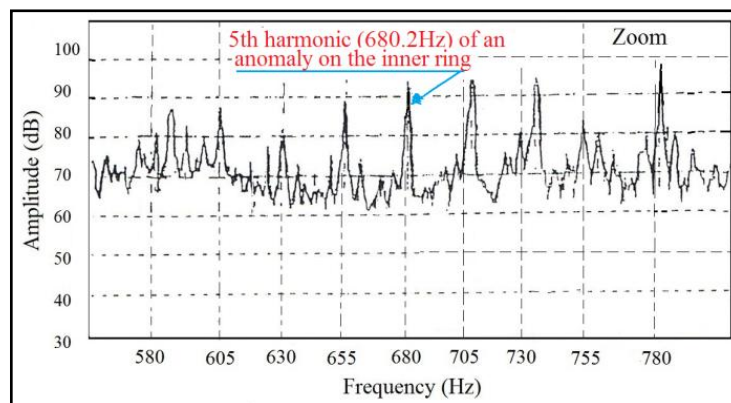


Fig.17 : Zoom mode spectrum of the bearing vibrations of induction machine of an anomaly on the inner ring .

The spectrum of this fig.18 Zoom mode structure of the resonance that appears around 780 Hz can be attributed to the 31st harmonic resonance of the rotation . $780.2 / 25 = 31.2$.

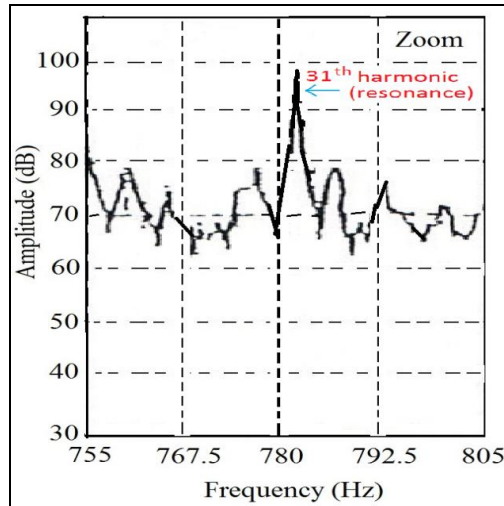


Fig.18 : Zoom mode spectrum around the bearing of the vibration resonance of the induction machine .

The fig.19 shows a simultaneous representation of the load torque spectrum in the case of anomaly and healthy case by displaying the lines and their characteristic frequencies.

The DSP of the torque on the shaft of the machine equipped with a rolling with an anomaly on the inner ring for a supply frequency of $f_s = 50$ Hz machine. We notice the appearance of harmonics located but also to a harmonic package centered around a combination of characteristic frequencies. This packet is characteristic harmonic torque variations due to the anomaly of the rolling.

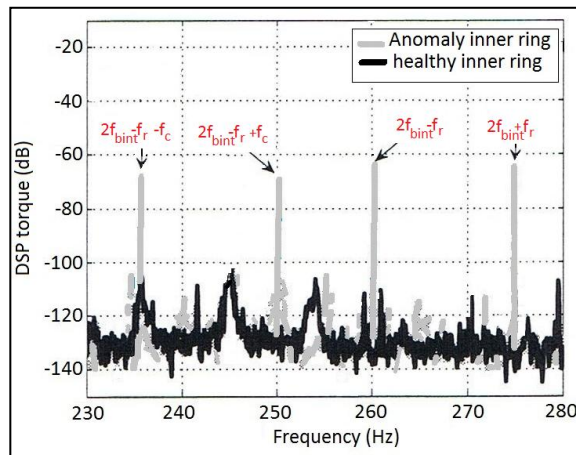


Fig.19: DSP torque for rolling healthy and contaminated

The results of experimental measurements of the amplitude of the torque harmonics at the frequency f_{bint} for different rotational speeds of the machine in the case of a localized defect on the inner ring and given by the following table1:

Rotation speed (rev / min)	300	600	900	1480
Amplitude of the harmonic torque (Nm)	0.0018	0.00215	0.00364	0.00656

Table 1: the amplitude of the harmonic torque based on the speed of the machine

2.1.interpretation:

- the evolution of the amplitudes of the harmonic components to $(605 + k25)$ Hz, $k = 0,1,2,3 , \dots$, frequency due to the passage of the balls on the notch .
- The evolution of amplitudes close to 100dB around 780 Hz that represent resonances of the structure.
- In addition, regardless of the type of anomaly or location , experimental studies show that the magnitude of the torque variations caused by rolling defects increases with the mechanical rotation speed . We can then see that the amplitude of this harmonic varies generally quadratically with the rotational speed.

3 . Effects of anomaly on the stator currents

The anomaly of the inner ring induces an oscillation of the torque at the frequency f_{osc} , which affect the stability of operating of the induction machine , this is shown by the experimental results given in Fig.20.

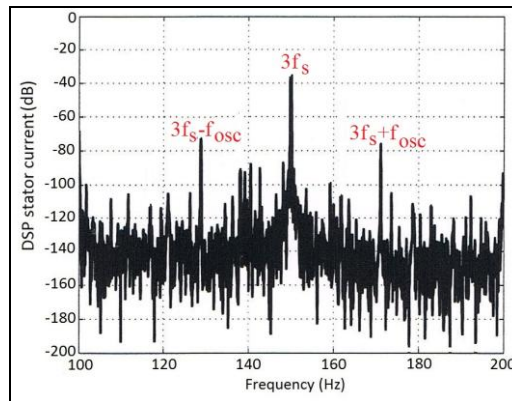


Fig.20: DSP of stator current

The torque oscillation primarily induce harmonics in stator currents of frequency of the lines in the spectrum $|fs \pm fosc|$ with $f_{osc} \approx 21\text{Hz}$.

VIII. Experimental bench

The experimental bench is composed of:

- A three-phase induction machine, the machine is controlled by an inverter ' OMRON ' , the rotor shaft is coupled to a DC generator which feeds into a rheostat to control the load.
- Characteristic of the induction machine:
 - Nominal power 4 Kw
 - Nominal speed 1480tr/min
 - Moment of inertia $J= 0.013\text{kgm}^2$
 - Number of pair of stove $P =2$
 - Rolling type ball SKF 6208, to a mechanical rotational frequency from $f_r = 25\text{Hz}$, les frequency outer ring , inner ring , and ball cage are respectively $f_{bext} =89.4\text{Hz}$, $f_{bint} =136\text{Hz}$, $f_c = 9.94\text{Hz}$ et $f_{bille} = 58.4\text{Hz}$.
- A light Microlog portable terminal for acquiring and storing from the sensor measurements.

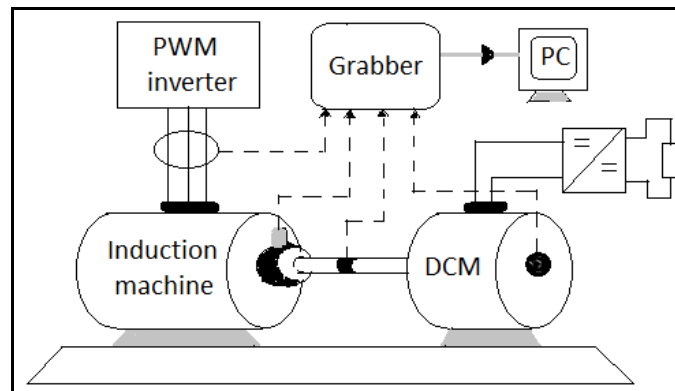


Fig.21: Schematic block diagram of the experimental bench

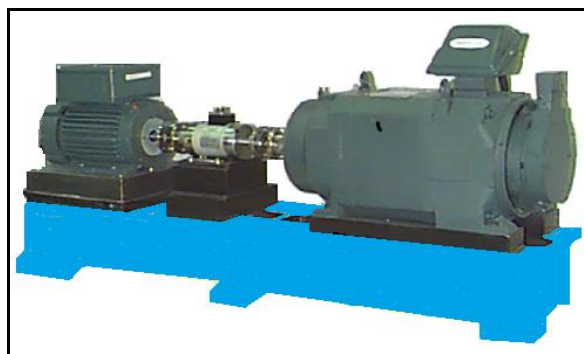


Fig.22: Photography machines of experimental bench

IX. Conclusion

The experimental measured kinematic frequencies may differ from theoretical ones, especially when the degradation of raceways is important. This difference may also result from insufficient or excessive load or accidental rotation of the fixed ring. Anomalies on the outer ring, the inner ring, the rolling elements, and the cage cause forces or movements, which generate vibrations measured by a sensor generally disposed on the non-rotating structure. The analysis of the signals delivered by the sensor provides elements in the temporal and frequency domains. These elements allow us to generate frequency components which are useful for the monitoring systems that facilitate diagnosis.

During the operating of the machine, a leakage current can pass through the rolling elements; electric arcs cause hot spots or mergers by rapid cooling after the metal quenching and craters are formed characterized by light spots with dark edges. For low currents alteration is less marked identified; it results in the grooves "indentation". To this effect, the Shocks produced by the passage of the balls on the indentation provoke the structures to respond through their own frequencies, which are particularly high. Thus, the evolution of the amplitudes of the received signal around these frequencies represents the resonances of the structure, detecting rolling anomalies by analysis of electrical current is relevant, but the major problem of current analysis is that mechanical defects are often embedded in noise or masked by strong electrical contribution, which does not allow a proper diagnosis from the electric current. To overcome these problems of resonance and noise, some methods, so-called high frequency resolution (HRF) were applied to help anomaly detection and diagnosis of the machines. However, the vibration monitoring method is often expensive because of the measurement chain. Through extensive researches conducted in order to compensate for vibration analysis, an approach based on the analysis and treatment of stator currents by intelligent modern techniques, has involved neural networks with genetic algorithm.

References

- [1]. N. Khalfaoui, M. S Salhi, H Amiri "Anomaly Detection in Induction Machines" 2nd International Conference on Automation, Control, Engineering and Computer Science; ACECS-2015 Sousse, Tunisia.
- [2]. B Trajin, J. Regnier, J. Faucher, Indicator for bearing fault detection in asynchronous motors using stator current spectral analysis, International Symposium on Industrial Electronics, Juin-Juillet 2008, pp. 570-575.
- [3]. F. Immovilli, C. Bianchini, M. Cocconcelli, A. Bellini, R. Rubini, "Bearing Fault Model for Induction Motor With Externally Induced Vibration," IEEE Trans. ind. Electron., vol.60, no. S, pp. 340S-341S, Aug. 2013. .
- [4]. B. Trajin, Détection automatique et diagnostic des défauts de roulements dans une machine asynchrone par analyse spectrale des courants statoriques, Conférence des jeunes chercheurs en génie électrique (JCGE), Décembre 2008, pp. 220-225.
- [5]. R. N. Andriamalala, H. Razik, L. Baghli, F. M. Sargos, Eccentricity fault diagnosis of a dual-stator winding induction machine drive considering the slotting effects, IEEE Transactions on Industrial Electronics, vol. 55, no. 12, D'ecembre 2008, pp. 4238-4251.
- [6]. R.BIGRET, J. L. FERON " Diagnostic- Maintenance disponibilité des machines tournantes " COLLECTION TECHNIQUES Ed. MASSON pp. 293-294-295.
- [7]. Y. Gritli, L. Zarri, C. Rossi, F. Filippetti, G.-A. Capolino, and D. Casadei, "Advanced diagnosis of electrical faults in wound rotor induction machines," IEEE Trans. Ind. Electron., vol. 60, no. 9, pp. 4012-4024, Sept. 2013.
- [8]. Javier A. Rosero, Antonio García , Luis Romeral ,and Jordi Cusidó "Fault Detection in Induction Machines Using Power Spectral Density in Wavelet Decomposition " IEEE TRANSACTIONS ON INDUSTRIAL ELECTRONICS, VOL. 55, NO. 2, FEBRUARY 2008
- [9]. A. Bellini, F. Filippetti, C. Tassoni, and G.-A.Capolino, "Advances in diagnostic techniques for induction machines," IEEE Trans. Ind. Electron., vol. 55, no. 12, pp. 4109-4126, 2008.
- [10]. Blodt, M. Chabert, J. Regnier, J. Faucher, Mechanical load fault detection in Induction motors by stator current time-frequency analysis, IEEE Transactions on Industry Applications, vol. 42, no. 6, Novembre - Décembre 2006, pp. 1454-1463.
- [11]. M. Blodt, P. Granjon, B. Raison, G. Rostaing, Models for bearing damage detection in induction motors using stator current monitoring, IEEE Transactions on Industrial Electronics, vol. 55, no. 4, Avril 2008, pp. 1813-1822.
- [12]. J .R Stack, T.G. Habetler and R.G. Harley, "Fault classification and fault signature production for rolling element bearings in electric machines, IEEE Trans. On Industry Applications, vol. 40 n. 3, pp.735-739, May- Jun. 2004.
- [13]. O. V. Thorsen, M. Dalva, "A survey of fault on induction motors in offshore oil industry, petrochemical industry, gas terminals, and oil refineries" IEEE Transactions on Industry Applications, Vol.31, no.5, pp.1186-1196, September1995.

- [14]. Jordi Cusidó, Luis Romeral, and Juan A. Ortega "Fault Detection in Induction Machines Using Power Spectral Density in Wavelet Decomposition" *IEEE TRANSACTIONS ON INDUSTRIAL ELECTRONICS*, VOL. 55, NO. 2, FEBRUARY 2008 , 633
- [15]. A. H. Bonnett, "Cause and analysis of Anti-Friction Bearing Failures in A.C Induction Motors" *IEEE Transactions on Industry Application*, pp 14 - 23, Sept/Oct 1993.
- [16]. Y. Gritli, L. Zarri, C. Rossi, F. Filippetti, G.-A. Capolino, and D. Casadei, "Advanced diagnosis of electrical faults in wound rotor induction machines," *IEEE Trans. Ind. Electron.*, vol. 60, no. 9, pp. 4012–4024, Sept. 2013.
- [17]. H. HEN AO, GÉRARD-ANDRÉ C. , M. FERNANDEZ-CABANAS, FIOREN ZO F. , CLAUDIO B. , ELIAS S. , REMUS P. , JORGE E., M. RIERA-GUASP, and S. HEDAYATI-KIA "Trends in Fault Diagnosis for Electrical Machines " June 2014 ©2014IEEE industrial electronics magazine 31.
- [18]. Javier A. Rosero, Antonio García , Luis Romeral ,and Jordi Cusidó "Fault Detection in Induction Machines Using Power Spectral Density in Wavelet Decomposition " *IEEE TRANSACTIONS ON INDUSTRIAL ELECTRONICS*, VOL. 55, NO. 2, FEBRUARY 2008 633
- [19]. A. Bellini, F. Filippetti, C. Tassoni, and G.-A. Capolino, "Advances in diagnostic techniques for induction machines," *IEEE Trans. Ind. Electron.*, vol. 55, no. 12, pp. 4109–4126, 2008.
- [20]. P. Zhang, Y. Du, T. G. Habetler, and B. Lu, "A survey of condition monitoring and protection methods for medium-voltage induction motors," *IEEE Trans. Ind. Applicat.*, vol. 47, no. 1, pp. 34–46, Jan./Feb. 2011